An Intestine-on-a-Chip Model of Plug-and-Play Modularity to Study Inflammatory Processes

Linda Gijzen[1]*, Diego Marescotti[2]* ID, Elisa Raineri[1], Arnaud Nicolas[1], Henriette L. Lanz[1], Diego Guerrera[2], Remko van Vught[1], Jos Joore[1], Paul Vulto[1], Manuel C. Peitsch[2], Julia Hoeng[2], Giuseppe Lo Sasso[2], and Dorota Kurek[1] ID

Abstract

Development of efficient drugs and therapies for the treatment of inflammatory conditions in the intestine is often hampered by the lack of reliable, robust, and high-throughput in vitro and in vivo models. Current models generally fail to recapitulate key aspects of the intestine, resulting in low translatability to the human situation. Here, an immunocompetent 3D perfused intestine-on-a-chip platform was developed and characterized for studying intestinal inflammation. Forty independent polarized 3D perfused epithelial tubular structures were grown from cells of mixed epithelial origin, including enterocytes (Caco-2) and goblet cells (HT29-MTX-E12). Immune cells THP-1 and MUTZ-3, which can be activated, were added to the system and assessed for cytokine release. Intestinal inflammation was mimicked through exposure to tumor necrosis factor-α (TNFα) and interleukin (IL)-1β. The effects were quantified by measuring transepithelial electrical resistance (TEER) and proinflammatory cytokine secretion on the apical and basal sides. Cytokines induced an inflammatory state in the culture, as demonstrated by the impaired barrier function and increased IL-8 secretion. Exposure to the known anti-inflammatory drug TPCA-1 prevented the inflammatory state. The model provides biological modularity for key aspects of intestinal inflammation, making use of well-established cell lines. This allows robust assays that can be tailored in complexity to serve all preclinical stages in the drug discovery and development process.

Keywords

intestinal inflammation, microfluidics, barrier integrity, plug-and-play complexity, high-throughput

Introduction

Intestinal inflammation is among the primary health indications in the Western world.[1] It comprises a range of diseases, from the less defined irritable bowel syndrome to full impairment of intestinal function in inflammatory bowel disease (IBD).[2] For this reason, preventive measures and treatments are major areas of focus for food, consumer goods, and pharmaceutical industries alike. The challenge in developing such preventive and therapeutic agents is that many of the processes involved in intestinal inflammation are still poorly understood. It is thought that environmental, genetic, immunological, and microbial factors play a role in intestinal inflammation.[3–5] Therefore, there have been increasing efforts to model the intestinal niche in its full complexity, including the push forward to even more personalized models. On the other hand, the in vitro modeling paradox dictates that cellular models should be made as simple, robust, and reproducible as possible, while still capturing the essence of the disease they are supposed to model. Depending on the industry and preventive/therapeutic modality, each phase of development places its own specific demands on the complexity and screenability of the

[1]Mimetas BV, Leiden, The Netherlands
[2]PMI R&D, Philip Morris Products S.A., Neuchâtel, Switzerland
*These authors contributed equally.

Corresponding Authors:
Dorota Kurek, Mimetas BV, JH Oortweg 19, Leiden, 2333CH, The Netherlands.
Email: d.kurek@mimetas.com

Giuseppe Lo Sasso, PMI R&D, Philip Morris Products S.A., Quai Jeanrenaud 5, Neuchâtel, CH-2000, Switzerland.
Email: Giuseppe.LoSasso@pmi.com

cell culture model. It is therefore of paramount importance that modeling platforms are available with full modularity with regard to the complexity of intestinal niche models. At the same time, these models need to be robust and screenable. Such modular platforms allow tailoring of complexity to the need of the respective phase in the development of a preventive or therapeutic modality.

Great progress has been made in advancing in vitro models representing the physiological and inflammatory processes in the gut through 3D,[6,7] organoid-based,[8–10] and microfluidic models.[11–13] Yu et al. showed that a 3D intestinal model that mimicked the shape and size of the human small intestinal villi by using collagen hydrogel scaffolds was more accurate than 2D cultures in predicting drug permeability. Furthermore, they demonstrated that cell differentiation varied along the villus, indicating the importance of the 3D architecture.[6] As shown by Noel et al., enteroids cultured as a monolayer in coculture with macrophages demonstrate enhanced barrier function and maturity, allowing access to both the apical and basal sides.[14] To develop a more powerful tool for understanding and investigating the human intestine, Kasendra et al. combined primary epithelial cells cultured as 3D organoids with a microfluidic chip. This model is exposed to fluid flow and can therefore be used to study nutrient digestion, mucus secretion, and the effect of drugs/substances on barrier integrity in a more in vivo-like situation.[11] Although these models are relevant and pertinent to the field of intestinal inflammation modeling, they lack the robustness or relationship to industry-adopted cellular standards and are generally not suitable for screening large libraries of compounds.[15]

Previously, we introduced an intestinal model comprising perfused tubules composed of the intestinal cell line Caco-2 in a microfluidic platform, the OrganoPlate.[16] The gut tubules showed accelerated cellular polarization, fundamental receptor expression, and tight junction formation in a robust and reproducible manner. Moreover, this gut-on-a-chip model was shown to be applicable for studying inflammatory processes in the gut.[17] The OrganoPlate platform allows the formation of 40 tubules in parallel and, owing to its standardized format, is compatible with a screening environment. The model comprises cells of the enterocyte phenotype, captured extracellular matrix (ECM) interaction and response to shear stress. Use of the industry-wide-adopted and broadly available cell line Caco-2 accelerated the uptake of the platform by various pharmaceutical companies.[17,18] However, because it was based on a single cell line, the model was limited in biological complexity.

In this study, we demonstrate that the biological complexity of the OrganoPlate-based intestinal tubular model can be expanded at will, here referred to as plug-and-play modularity. We expanded the tubular Caco-2 enterocyte model with the mucus-secreting HT29-MTX-E12 cells containing a goblet cell phenotype. Furthermore, we added the immune-competent cells THP-1 and MUTZ-3 to the basal side of the epithelium. To mimic intestinal inflammation, we exposed the model to various cytokines and assessed their effects by measuring transepithelial electrical resistance (TEER) and proinflammatory cytokine secretion in both compartments. Finally, we exposed the model to the well-known anti-inflammatory drug TPCA-1 and showed that the drug can prevent inflammation.

Materials and Methods

Cell Culture

The human colon adenocarcinoma cell line Caco-2 (86010202; Sigma-Aldrich, St. Louis, MO) was cultured in T75 flasks in Eagle's minimum essential medium (EMEM; 30-2003; ATCC, Manassas, VA) supplemented with 10% fetal bovine serum (FBS; 16140-071; Thermo Scientific, Waltham, MA), 1% nonessential amino acids (NEAA; 11140-050; Life Technologies, Carlsbad, CA), and 1% penicillin–streptomycin (P4333; Sigma-Aldrich). The human colon cell line HT29-MTX-E12 (12040401; Sigma-Aldrich) was cultured in T75 flasks in Dulbecco's modified Eagle's medium (DMEM; D6546, Sigma-Aldrich) supplemented with 10% FBS (16140-071; Thermo Scientific), 1% NEAA (11140-050; Life Technologies), 1% GlutaMAX (35050-061; Thermo Scientific), and 1% penicillin–streptomycin (P4333; Sigma-Aldrich). The human acute monocytic leukemia cell line THP-1 (Tib-202; ATCC) was cultured in T25 flasks in Roswell Park Memorial Institute 1640 medium (RPMI; R0883, Sigma-Aldrich) supplemented with 10% FBS (16140-071; Thermo Scientific), 1% GlutaMAX (35050-061; Thermo Scientific), and 1% penicillin–streptomycin (P4333, Sigma-Aldrich). THP-1 cells cultured in six-well plates were differentiated toward macrophages by exposure to 5 ng/mL PMA (phorbol 12-myristate 13-acetate) in the medium. After 72 h, the medium was replaced with standard culture medium, and the cells were further incubated for 24 h and then trypsinized with TrypLE Express (12604-013; Life Technologies) for seeding in the OrganoPlate. The human acute myelomonocytic leukemia cell line MUTZ-3 (ACC 295; DSMZ, Braunschweig, Germany) was cultured in T25 flasks in alpha-minimum essential medium (M4526; Sigma-Aldrich) supplemented with 20% FBS (16140-071; Thermo Scientific), 1% GlutaMAX (35050-061; Thermo Scientific), 1% penicillin–streptomycin (P4333; Sigma-Aldrich), and a 10% conditioned medium of confluent layers of 5637 cells (HTB-9; ATCC). The cells were cultured in a humidified incubator (37 °C; 5% CO_2) and maintained by adding fresh medium every 2–3 days. All experiments were performed with Caco-2, HT29-MTX-E12, THP-1, and MUTZ-3 cells between passages 53 and 60, 53 and 58, 6 and 14, and 6 and 9,

respectively. The cells were routinely tested for mycoplasma contamination and found negative.

OrganoPlate Culture

This study employed the OrganoPlate three-lane (Mimetas BV, Leiden, the Netherlands) with 400×220 μm (w × h) channels. The phaseguides were 100×55 μm (w × h) in dimension. Before loading ECM, each observation window was filled with 50 μL od Hank's balanced salt solution (HBSS) to prevent dehydration and provide optical clarity. Next, 2 μL of ECM composed of 4 mg/mL collagen-I (Cultrex 3D collagen-I Rat Tail; 5 mg/mL; 3447-020-01; AMS Biotechnology, Abingdon, UK), 100 mM HEPES (15630-122; Thermo Scientific), and 3.7 mg/mL NaHCO$_3$ (S5761; Sigma-Aldrich) was dispensed into the gel inlet. After incubation for 15 min at 37 °C, 20 μL of HBSS was added on top of the gel inlet, and the plate was incubated overnight in a humidified incubator at 37 °C. Caco-2 and HT29-MTX-E12 cells were trypsinized with 0.25% trypsin (15290-046; Thermo Scientific) and 0.53 mM ethylenediaminetetraacetic acid (AM9260G; Thermo Scientific), aliquoted, and pelleted (200g; 5 min). A suspension of Caco-2 and HT29 cells (concentration, 1×10^7 cells/mL) was prepared in a ratio of 6:1 in EMEM-supplemented Caco-2 medium. Subsequently, a 2 μL cell suspension was injected into the inlet of the top medium channel, after which 50 μL of medium was added to the same well. The OrganoPlate was placed on its side for 3.5 h at 37 °C to allow the cells to sediment and attach to the ECM. Next, an additional 50 μL of culture medium was added to each of the remaining inlets and outlets of the top and bottom medium channels. Subsequently, the OrganoPlate was placed horizontally in a humidified incubator (37 °C; 5% CO$_2$) on an interval rocker switching between a $+7°$ and $-7°$ inclination every 8 min (OrganoFlow; Mimetas BV), allowing bidirectional flow. With these settings, a mean flow rate of 2.02 μL/mL could be achieved, resulting in a mean shear stress of 0.13 dyne/cm^2 and thereby closely mimicking physiological levels of intestinal epithelial shear stress ranging between ~0.002 and 0.08 dyne/cm^2.[19–21] The medium was refreshed every 2–3 days. On day 4 of culture, differentiated THP-1 and MUTZ-3 cells were collected, aliquoted, and pelleted (300g; 5 min). A suspension of THP-1 and MUTZ-3 cells (concentration, 3×10^6 cells/mL) was prepared in a ratio of 1:1 in EMEM-supplemented Caco-2 medium. The medium in the bottom perfusion channel of each chip was aspirated, and 2 μL of the cell suspension was injected into the inlet of the bottom medium channel. Because the channels were wet, and the capillary force was lost, the cells were forced through the channel by pipetting 0.5 μL of the cell suspension from the outlet into the inlet. This process was repeated three times, after which the OrganoPlate was placed on its side for 30 min at 37 °C to allow the immune cells to attach to the ECM. Subsequently, the medium present in the top medium channel was aspirated, and 50 μL of fresh EMEM-supplemented Caco-2 medium was added to all inlets and outlets of the top and bottom medium channels. The plate was again placed horizontally on the interval rocker. Experiments involving compound exposure for inducing or preventing inflammation were all performed on day 4 or 5 of culture.

Immunohistochemical Analysis

Cultures in the OrganoPlate were fixed with 3.7% formaldehyde (252549; Sigma-Aldrich) in phosphate-buffered saline (PBS; 20012068; Life Technologies) for 10 min, then washed twice for 5 min with PBS, and permeabilized with 0.3% Triton X-100 (T8787; Sigma-Aldrich) in PBS for 10 min. Next, the cultures were washed with 4% fetal calf serum (FCS; 16140-071; Thermo Scientific) in PBS and incubated with blocking solution (2% FCS, 2% bovine serum albumin [BSA; A2153; Sigma-Aldrich], and 0.1% Tween-20 [P9416; Sigma-Aldrich] in PBS) for 40 min. The cells were then incubated with primary antibodies for 60 min at room temperature (RT), washed twice, incubated with secondary antibodies for 30 min at RT, and washed twice with 4% FCS in PBS. The following antibodies were used for immunohistochemical analysis: mouse anti-acetylated tubulin (1:2000; T6793; Sigma-Aldrich), rabbit anti-occludin (1:100; 71-1500; Thermo Scientific), mouse anti-ezrin (1:50; 610602; BD Biosciences, San Jose, CA), rabbit anti-ZO-1 (1:125; 617300; Invitrogen, Carlsbad, CA), rabbit isotype (86199; Life Technologies), mouse isotype (86599, Life Technologies), goat anti-rabbit AlexaFluor 488 (1:250; A11008; Thermo Scientific), and goat anti-mouse AlexaFluor 555 (1:250; A21422; Life Technologies). Finally, the nuclei were stained with Hoechst 33342 (H3570; Thermo Scientific) and the cells were stored in PBS. The cultures were imaged with the ImageXpress Micro XLS-High Content Imaging System (Molecular Devices, San Jose, CA).

TEER Measurement

The TEER of the cultures in the OrganoPlate was measured by using an automated multichannel impedance spectrometer (OrganoTEER; Mimetas BV). An electrode board containing gold electrodes that matched the OrganoPlate three-lane layout was cleaned with 70% ethanol an hour before measurement. Prior to measurement, 50 μL of Caco-2 culture medium was added to all inlets and outlets, and the OrganoPlate was placed on a rocker platform (8 min; 7°) for 30 min in a humidified incubator (37 °C; 5% CO$_2$) for equilibration. Subsequently, the OrganoPlate was placed in the OrganoTEER device, and point impedance measurements were performed with a frequency range of 10 Hz to 1 MHz (41 points; precision, 0.2) at RT. The

corresponding software automatically generated the TEER values per chip in ohms (Ω). These values were normalized to ohm-square centimeters by multiplication with the surface area of the tubule–ECM interface (0.0057 cm^2).

Gene Expression Analysis

Epithelial tubes composed of Caco-2 and HT29-MTX-E12 cells were harvested from the top medium channel of the OrganoPlate by using RLT lysis buffer (79216; Qiagen, Hilden, Germany). RNA was extracted by using the RNeasy Micro kit (74004; Qiagen) and purified in accordance with the manufacturer's protocol. M-MLV reverse transcriptase (28025013; Thermo Scientific) was used to synthesize complementary DNA by following the manufacturer's protocol. The following probes were used in this study: MUC2 (forward: 5′-ACTGCGAGCAGTGTGTCTGT-3′, reverse: 5′-AGGTGTACGTCTTCCCATCG-3′), MUC5AC (forward: 5′-AGGCCTGTGTCTGCACCTAC-3′, reverse: 5′-CAGG GGTAGACCCTCCTCTC-3′), MUC12 (forward: 5′-CCTG GAAACCTTAGCACCAG-3′, reverse: 5′-GACAGACGC ATTGTTTTCCAT-3′), MUC13 (forward: 5′-TCCTCCTCA GATTACCAAGCA-3′, reverse: 5′-GTTTAGGGTGCTGG TCTCCA-3′), MUC16 (forward: 5′-GGTGGACATCCATG TGACAG-3′, reverse: 5′-TCCTAGGTTGGTGATGGTGA-3′), MUC20 (forward: 5′-TCCCTCCGACTACAACCAA C-3′, reverse: 5′-ACCTCCATTTTCACCTGCAC-3′), and ACTB (forward: 5′-CTCTTCCAGCCTTCCTTCCT-3′, reverse: 5′-AGCACTGTGTTGGCGTACAG-3′). Quantitative PCR was performed with the LightCycler 96 system (Roche Molecular Systems Inc., Pleasanton, CA) by using FastStart Essential DNA Green Master (06402712001, Roche). Data were analyzed with the corresponding software, and the expression levels of β-actin were used as the reference for normalization.

Alcian Blue Staining

Cultures in the OrganoPlate were fixed with 0.1% glutaraldehyde (G5882; Sigma-Aldrich) in HBSS (H6648; Sigma-Aldrich) for 20 min at RT and then washed three times with HBSS. Next, the cultures were exposed to 1% Alcian blue (B8438; Sigma-Aldrich) prepared in 3% acetic acid (A6238; Sigma-Aldrich; pH 2.5) and incubated for 2 h by placing the OrganoPlate on a rocker platform (8 min; 7°). Alcian blue was used to detect acidic mucous substances in the tubular structures. Subsequently, the cells were washed once with 3% acetic acid and two times with HBSS and then stored in HBSS. Image acquisition was performed by using the EVOS FL Auto 2 Imaging System (Thermo Scientific).

Cytokine Kinetics in the OrganoPlate

To analyze the diffusion of potentially inflammatory cytokines either released by the immune cells or added to the

system, the kinetics of several cytokines in the OrganoPlate was assessed. A total of 2 µL of ECM composed of 4 mg/mL collagen-I, 100 mM HEPES, and 3.7 mg/mL NaHCO$_3$ was dispensed into the gel inlet. After incubation for 15 min at 37 °C, 20 µL of HBSS was added on top of the gel inlet, and the plate was incubated overnight in a humidified incubator at 37 °C. Next, 50 µL of a cytokine mixture composed of 0.5 mg/mL fluorescein isothiocyanate (FITC)–dextran (150 kDa; 46946; Sigma-Aldrich), 100 ng/mL tumor necrosis factor-α (TNFα) (210-TA-020; R&D Systems, Minneapolis, MN), 100 ng/mL interleukin (IL)-1β (11340015; Immunotools, Friesoythe, Germany), and 20 ng/mL IL-8 (11349084; Immunotools) in Caco-2 complete medium was added to the inlet and outlet of each top medium channel in the OrganoPlate three-lane. In the bottom medium channel, 50 µL of Caco-2 complete medium was added to the inlet and outlet. The OrganoPlate was then placed on a rocker platform (8 min; 7°), and medium was collected from the apical (top) and basolateral (bottom) compartments after 0.5, 1, 2, 6, 24, and 72 h. Then, IL-8, TNFα, and IL-1β present in the medium were quantified by using the human IL-8/CXCL8 DuoSet ELISA kit (DY208; R&D Systems), human IL-1 beta/IL-1F2 DuoSet ELISA kit (DY201-05; R&D Systems), and human TNF alpha DuoSet ELISA kit (DY210-05; R&D systems), respectively, in accordance with the manufacturer's protocol. Additionally, the diffusion of FITC–dextran was assessed by fluorescent imaging with ImageXpress XLS Micro (Molecular Devices).

Immune Cell Functionality in the OrganoPlate

To determine the functionality of the immune cells in the OrganoPlate, 3000 or 6000 differentiated THP-1 and/or MUTZ-3 cells were seeded in the top compartment of a three-lane chip in mono- or coculture against a collagen-I ECM. The cells were exposed to 0, 1, 10, and 100 ng/mL lipopolysaccharide (LPS; L2630; Sigma-Aldrich) in the apical (top) compartment. Medium was collected from the apical and basolateral compartments 24, 48, and 72 h after exposure, and the concentration of IL-8 (CXCL8) was determined by using the human IL-8/CXCL8 DuoSet ELISA kit (DY208; R&D Systems) in accordance with the manufacturer's protocol. The absorbance of the samples at 450 nm was measured by using the Multiskan FC Microplate Photometer (Thermo Scientific).

Induction of Inflammation

The tetraculture model in the OrganoPlate was exposed to 300 ng/mL TNFα (210-TA-020; R&D Systems) on the basolateral side (bottom medium channel) or 200 ng/mL TNFα and IL-1β (11340015, Immunotools) on the apical and basolateral sides (top and bottom medium channels) on day 4 of culture. This was done by replacing the cell culture medium in the inlets and outlets of the bottom and/or top

medium channels with 50 µL of medium containing the inflammatory trigger(s). TNFα and IL-1β were dissolved in sterile PBS and sterile Millli-Q water, respectively. The cultures were exposed to the cytokines for 72 h on a rocker platform for interval measurement of phase-contrast imaging, barrier integrity (fluorescent probe assay and TEER measurement), and cytokine secretion. Finally, the cultures in the OrganoPlate were fixed with 3.7% formaldehyde and stored in PBS at +4 °C.

Cytokine Secretion Analysis

Media in the top and bottom medium channels were collected, and samples from the inlets and outlets were pooled. CXCL8 was determined by using the human IL-8/CXCL8 DuoSet ELISA kit (DY208; R&D Systems) in accordance with the manufacturer's protocol. The absorbance of the samples at 450 nm was measured by using the Multiskan FC Microplate Photometer (Thermo Scientific).

Barrier Integrity Assay in the OrganoPlate

All medium was aspirated from the chips, and 20 µL of medium without a fluorescent compound was added to the basal side of the chips (inlets and outlets of the gel channel and the bottom medium channel). Medium containing 0.5 mg/mL tetramethylrhodamine isothiocyanate (TRITC)–dextran (4.4 kDa; T1037; Sigma-Aldrich) was added to the top medium channel, which contained an epithelial tubule of Caco-2 and HT29-MTX-E12 cells. Subsequently, leakage of the fluorescent dye from the lumen of the tube into the ECM compartment was imaged over time with ImageXpress XLS Micro (Molecular Devices). The ratio between fluorescent signals in the basal and apical compartments of the tube was analyzed by using FiJi.[22]

Compound Exposure for Preventing Inflammation

To determine the protective effect of anti-inflammatory compounds on an inflamed tetraculture, cells in the OrganoPlate were pretreated with 1 µM TPCA-1 (2559; Tocris, Bristol, UK) or budesonide (100, 500, or 1000 nM; B7777; Sigma-Aldrich) on both the apical and basolateral sides or only on the basolateral side for 6 h, respectively. Subsequently, the medium was replaced with medium containing the cytokine triggers (300 ng/mL TNFα on the basolateral side or 200 ng/mL TNFα and IL-1β on both sides) and the anti-inflammatory compound. The cultures were placed on a rocker platform and exposed to the cytokines and anti-inflammatory compound for interval measurement (24, 48, and 72 h) of phase-contrast imaging, barrier integrity (fluorescent probe assay and TEER measurement), and cytokine secretion. Finally, the cultures in the OrganoPlate were fixed with 3.7% formaldehyde.

Statistics and Data Analysis

Image analysis was performed by using FiJi. Data analysis was performed by using Excel (Microsoft Corp., Redmond, WA) and GraphPad Prism 6 (GraphPad Software Inc., San Diego, CA). All data are expressed as the mean ± standard deviation (SD) of values from at least three individual chips ($n = 3$). Statistical analysis was performed by two-way analysis of variance with Tukey's multiple comparisons test, unless stated otherwise. Statistical significance was considered at $p < 0.05$. Datasets, detailed protocols, and additional data visualizations are available on the INTERVALS platform at https://doi.org/10.26126/intervals.o3gtmh.1.

Results

Establishment of a Multicellular Intestine-on-a-Chip Model

To establish a 3D in vitro multicellular microfluidic intestinal model, we adapted a previously established intestine-on-a-chip model in which polarized and leak-tight Caco-2 tubules had been achieved.[16] The microfluidic device used in this study, the OrganoPlate three-lane, contains 40 microfluidic chips embedded in a standard 384-well microtiter plate format (**Fig. 1A**). Each chip comprises three adjacent culture channels linked to 9 wells of the microtiter plate, which serve as channel inlets and outlets. The channels join at the center of the chip, where they are separated by two capillary pressure barriers called phaseguides. The center well also serves as an observation window for monitoring the culture and for readout purposes.

Additional cell types were added to the system to better recapitulate the intestinal physiology and increase the model complexity and cell-to-cell interaction. The enterocyte-like Caco-2 tubule phenotype was enriched by addition of the mucus-producing HT29-MTX-E12 cells.[23,24] To explore the usability of the platform for modeling intestinal inflammation, two immune cell components were incorporated into the chip: intestinal macrophages and dendritic cells, which have been shown to be involved in the pathogenesis of intestinal inflammation.[25] This was achieved by employing THP-1 cells (mimicking the macrophage phenotype) and MUTZ-3 cells (mimicking dendritic cells).[26] The methodology for establishing a membrane-free multicellular intestine-on-a-chip model is schematically illustrated in **Figure 1B**. Depending on the research question, either a simple or a more complex coculture can be assembled. The patterning of a collagen-I gel in the middle channel of each chip is the first step in setting up the model for all culture configurations. The liquefied ECM enters the channels by capillary action and, owing to the meniscus-pinning effect of the phaseguides, it does not overflow into the adjacent channels. After ECM gelation, a single-cell mixture of
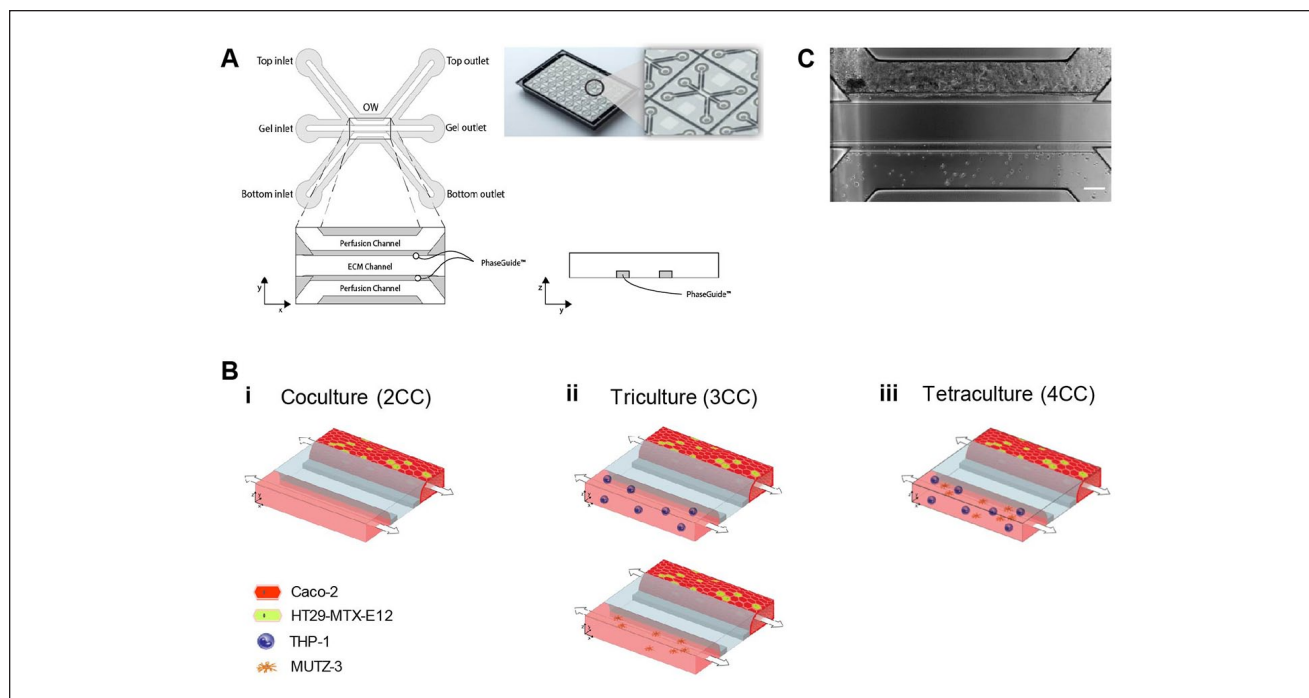
Figure 1. Establishment of a multicellular intestine-on-a-chip model in the OrganoPlate. (**A**) Bottom view of the OrganoPlate three-lane platform with 40 microfluidic cell culture chips embedded in a standard 384-well microtiter plate. Zoom-in image and schematic image showing the horizontal and vertical views of one microfluidic chip consisting of three channels: two medium perfusion channels and a gel channel in the middle separated by phaseguides. These channels join in the center of the chip and are located in the observation window (OW) well. (**B**) Schematic representation of the seeding strategy for establishing a biological modular model consisting of a coculture (i), triculture (ii), or tetraculture (iii) intestine-on-a-chip. After patterning a collagen-I ECM (light blue) into the middle channel of the chip, between two phaseguides, a mixture of Caco-2 and HT29-MTX cells is seeded in the top channel. By placing the plate on its side, the cells are allowed to settle against the ECM. Upon starting medium perfusion flow, the cells start to grow into a tubular structure, covering the channel and ECM surface. Once a confluent tubular structure has been obtained, usually on day 4 of culture, differentiated THP-1 and/or MUTZ-3 cells are added to the bottom perfusion channel. After an attachment period against the ECM, medium perfusion flow is restarted. (**C**) Phase-contrast image of the intestine-on-a-chip model comprising the tubular structure of Caco-2 and HT29-MTX cells in the top compartment and differentiated THP-1 and MUTZ-3 cells in the bottom compartment on day 4 of culture. Scale bar in white = 200 μm.

Caco-2 and HT29-MTX-E12 cells in medium (6:1 ratio) is loaded into the top medium channel, and the cells are allowed to attach to the ECM by placing the plate on its side in the vertical position. This step is the same for the coculture (2CC), triculture (3CC), and tetraculture (4CC) platforms (**Fig. 1Bi–iii**). Subsequently, the plate is placed horizontally on an interval rocker platform to induce perfusion flow through gravity-driven liquid leveling between the reservoirs. Upon perfusion flow, the cells start to proliferate and line all surfaces of the perfusion channel. After establishment of a confluent tubular structure, either a single-cell suspension of differentiated THP-1 or MUTZ-3 cells in medium (**Fig. 1Bii**) or a combination of both cells (1:1 ratio) is loaded into the bottom medium channel (**Fig. 1Biii**), and the cells are allowed to attach to the ECM. Both the apical (lumen of the tube) and basolateral (accessible from the bottom medium channel) sides can be perfused with medium, exposed to compounds, and assessed for

cytokine release. The culture conditions for the intestinal tetraculture model were optimized by testing different parameters such as seeding density and configuration of cells relative to each other (**Suppl. Fig. S1A–D**). We have thus established a microfluid-based multicellular intestine-on-a-chip model with a robust and reproducible phenotype (**Fig. 1C, Suppl. Fig. S2A**).

Characterization of the Intestinal Model

To examine the physiological relevance of mimicking the intestinal microenvironment, the expression of key markers in the tetraculture model in the OrganoPlate was assessed by using an immunofluorescence-based approach in combination with high-content microscopy. A 3D reconstruction of a gut tubule consisting of Caco-2 and HT29-MTX-E12 cells shows a tubular structure with cells lining the ECM and walls of the medium channel, which indicates the
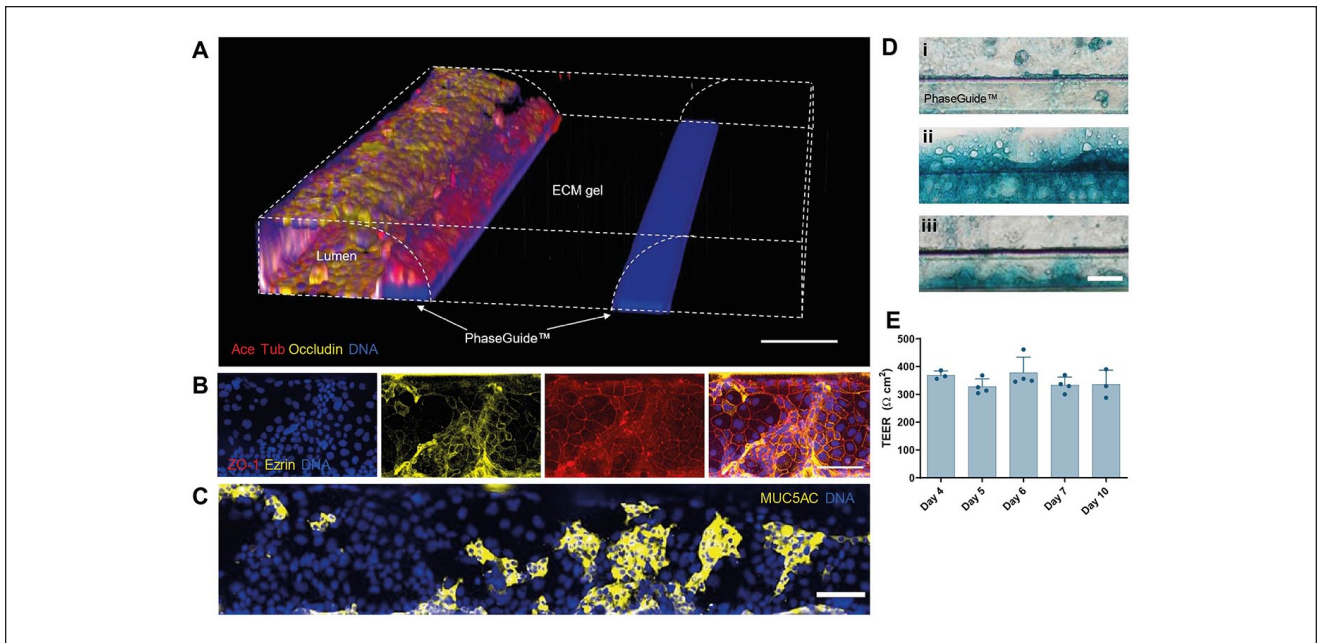
Figure 2. Characterization of the tetraculture intestine-on-a-chip model in the OrganoPlate. (**A**) 3D reconstruction of a confocal z-stack at 10× magnification, showing a tubular epithelial structure of Caco-2 and HT29-MTX cells against a collagen-I ECM patterned in the middle compartment. The tube was stained for acetylated tubulin (red), occludin (yellow), and DNA (blue). (**B**) Representative immunofluorescent max projections (20× magnification) of the epithelial tube in the tetraculture on day 4, stained for ezrin (yellow), zonula occludens 1 (ZO-1; red), and DNA (blue). (**C**) Max projection of a stained tubular structure of Caco-2 and HT29-MTX cells in the top compartment of an OrganoPlate three-lane on day 4 of culture. The cells are stained for mucin 5AC (MUC5AC; yellow) and DNA (blue). Scale bar in white = 50 μm. (**D**) Alcian blue staining of a monoculture of Caco-2 (i) or HT29-MTX cells (ii) or a coculture of Caco-2 and HT29-MTX cells (iii) in an OrganoPlate three-lane on day 4. Acidic glycosaminoglycans produced and secreted by the cells into the lumen of the tube are visualized in blue. (**E**) Epithelial tubule barrier function in the tetraculture model was assessed by measuring TEER at multiple days, showing stable barrier formation from day 4 until day 10 (*n* = 4). All cultures were fixed on day 4 of culture. Scale bars in white = 100 μm (**A,B**), 50 μm (**C**), and 25 μm (**D**).

presence of a clear lumen with access to both the apical and basolateral sides (**Fig. 2A**). Furthermore, the coculture of Caco-2 and HT29-MTX-E12 cells displays brush-border formation and tight junctions, as shown by the expression of ezrin and ZO-1, respectively (**Fig. 2B**). To further examine functional barrier formation in the coculture, the barrier integrity of the culture was assessed by using a fluorescent probe (the 4.4 kDa TRITC–dextran probe), which was perfused into the lumen of the gut tubule. Leakage of the fluorescent probe into the ECM compartment was determined and normalized to the fluorescence in the lumen of the tube. As shown in **Supplemental Figure S2B**, the fluorescent probe was retained in all chips filled with the coculture, indicating the presence of an intact and leak-tight barrier.

Additionally, the TEER of the coculture was measured from days 4 to 10 of culture. The epithelial coculture tubules showed a TEER of 369 ± 15.4 Ωcm^2 on day 4 of culture, and this TEER remained stable up to day 10 (**Fig. 2E**). Furthermore, the functionality of the mucus-producing HT29-MTX-E12 cells in the intestinal model was confirmed by assessing gene expression and mucus production. Expression of the genes *MUC2, MUC5AC, MUC12,*

MUC13, MUC16, and *MUC20* was observed after 24 h (day 4), 48 h (day 5), and 72 h (day 6) of coculture (**Suppl. Fig. S1E**). The results of immunofluorescence staining of MUC5AC showed clear local expression of mucin in the coculture tubule (**Fig. 2C**).

Finally, tubular structures composed of only Caco-2 or HT29-MTX-E12 cells and a coculture of both cells in the OrganoPlate were stained with Alcian blue on day 4 of culture. As shown in **Figure 2D**, the monoculture of HT29-MTX-E12 cells (**Fig. 2Dii**) showed the highest intensity of staining. Interestingly, the Caco-2 monoculture (**Fig. 2Di**) also displayed staining of mucins, but to a lower extent than the HT29-MTX-E12-containing tubules. Finally, the coculture of Caco-2 and HT29-MTX-E12 cells showed an intermediate level of staining (**Fig. 2Diii**). In summary, these results showed that leak-tight, polarized, and mucus-producing tubular structures were obtained in the OrganoPlate.

Mimicking Intestinal Inflammation

In order to obtain a model that closely reflects the physiological cellular composition of the intestine, immune cells

were added to the bottom perfusion channel of the OrganoPlate three-lane to obtain the triculture or tetraculture intestine model. First, the functionality of both THP-1 and MUTZ-3 cells in the OrganoPlate was determined. Mono- and cocultures of the immune cells (3000 or 6000 cells) seeded in the OrganoPlate were exposed to different concentrations of LPS and assessed for the release of IL-8. The individual and combined contributions of the different cell types to IL-8 release were assessed after 24, 48, and 72 h of exposure (**Suppl. Fig. S3**). IL-8 release was higher in both monoculture conditions with 6000 cells than in cultures with 3000 cells (**Suppl. Fig. S3A,B**). Furthermore, higher levels of IL-8 were detected in the apical (top) compartment, where the cells were located, than in the basolateral compartment. Combining THP-1 and MUTZ-3 cells in a coculture resulted in a synergistic release of IL-8 into the medium in the apical compartment; this IL-8 release was higher when more cells were present in the system (**Suppl. Fig. S3C**). Thus, to ensure robust and measurable IL-8 release, 6000 cells/chip was considered the optimal seeding density for both immune cell types.

Additionally, LPS was also tested as an inducer of inflammation in the epithelial tubule and showed no effect on barrier integrity or IL-8 release (**Suppl. Fig. S4A,B**). Interestingly, the proinflammatory cytokines involved in intestinal inflammation[27] (TNFα[28] and IL-1β) either alone or together caused a substantial decrease in barrier integrity, as revealed by the TEER values (**Suppl. Fig. S5A**). Next, the diffusion of inflammatory cytokines—either released by the immune cells or added to the system—was determined by assessing their kinetics in the OrganoPlate. To this end, IL-8, TNFα, and IL-1β were added—together with the 150 kDa FITC–dextran probe—to the top (apical) medium compartment of a chip containing only ECM in the middle compartment (**Suppl. Fig. S5B**). Real-time imaging at intervals showed diffusion of the dye over time in the chip (**Suppl. Fig. S5C**). The fluorescence images showed that 82.7% of the FITC–dextran was detectable in the bottom perfusion channel after 72 h (**Suppl. Fig. S5D**). Cytokine analysis of medium samples containing IL-8, TNFα, and IL-1β revealed that 16.7%, 10.1%, and 8.5% of these cytokines had reached the bottom medium channel after 72 h, respectively (**Suppl Fig. S5E–G**). Overall, these results indicate that the cytokines can cross the collagen-I ECM by passive diffusion and reach the other compartment.

Knowing this, we proceeded to mimic intestinal inflammation in the model by exposing the tetraculture model to TNFα and IL-1β on both the apical and basolateral sides for 72 h on days 4–5 of culture (**Fig. 3A**). This inflammation cocktail and exposure strategy were found to be the most effective in inducing a decrease in barrier integrity and an increase in IL-8 expression in all seeding conformations (**Suppl. Fig. S6**). Phase-contrast images revealed that the morphology of the Caco-2 and HT29-MTX-E12 coculture

was not affected by the cytokine cocktail or TNFα alone in comparison with control chips (**Fig. 3B, Suppl. Fig. S7B**). The integrity of the epithelial coculture barrier was assessed on the basis of fluorescent probe leakage and TEER values. To this end, medium containing the 4.4 kDa TRITC–dextran probe was added to the lumen of the tube and assessed for leakage into the adjacent ECM channel. The cell-free control showed clear leakage of the fluorescent dye into the ECM channel (**Suppl. Fig. S8**). In contrast, chips that contained the tetraculture and were exposed to inflammatory triggers (TNFα or TNFα and IL-1β) showed retention of the fluorescent dye within the lumen of the tube. This result was comparable to that observed in chips that were not exposed to the cytokines. These results indicate that the epithelial barrier remains leak-tight even when exposed to inflammatory triggers for 72 h. Interestingly, TEER measurements revealed that exposure to cytokines produced a significant drop in TEER over time relative to the TEER observed in nonexposed chips (**Fig. 3C, Suppl. Fig. S7C**). After 72 h, exposure to TNFα or TNFα and IL-1β led to a decrease in TEER of 29.7% or 45.6%, respectively, relative to the TEER in nonexposed cultures. Furthermore, the TEER values of nonexposed chips increased over time, indicating increased barrier integrity. Overall, TEER measurement of the cultures produced more sensitive and accurate observations than the fluorescent barrier integrity assay. Subsequently, IL-8 release in the apical and basolateral compartments was assessed. **Figure 3D** and **Supplemental Figure S7D** show that triggered cultures released significantly higher levels of IL-8 into the medium than nontriggered cultures. Furthermore, the effect of combining THP-1 and MUTZ-3 cells on IL-8 release in cultures exposed to both TNFα and IL-1β can be observed in **Supplemental Figure S6**.

Preventing Intestinal Inflammation

Finally, to test the applicability of the model for screening anti-inflammatory compounds, the tetraculture was pretreated with 1 μM TPCA-1 for 6 h prior to addition of the inflammatory cocktail (TNFα and IL-1β) in the extended presence of the compound (**Fig. 4A**). TEER measurements revealed a significant difference in TEER between the treated and nontreated chips in the presence of TNFα and IL-1β after 72 h of exposure. TPCA-1-treated cultures triggered with TNFα and IL-1β showed TEER values similar to those of the vehicle control (**Fig. 4B**). Furthermore, the IL-8 levels in medium samples from the apical and basolateral sides were assessed 24, 48, and 72 h after exposure. Cultures exposed to TNFα and IL-1β showed increased IL-8 secretion (both apical and basolateral sides) relative to nontreated cultures (**Fig. 4C**). Of note, TPCA-1 pretreatment significantly hampered IL-8 release, as evident upon comparing TPCA-1-treated cells with cytokine-treated
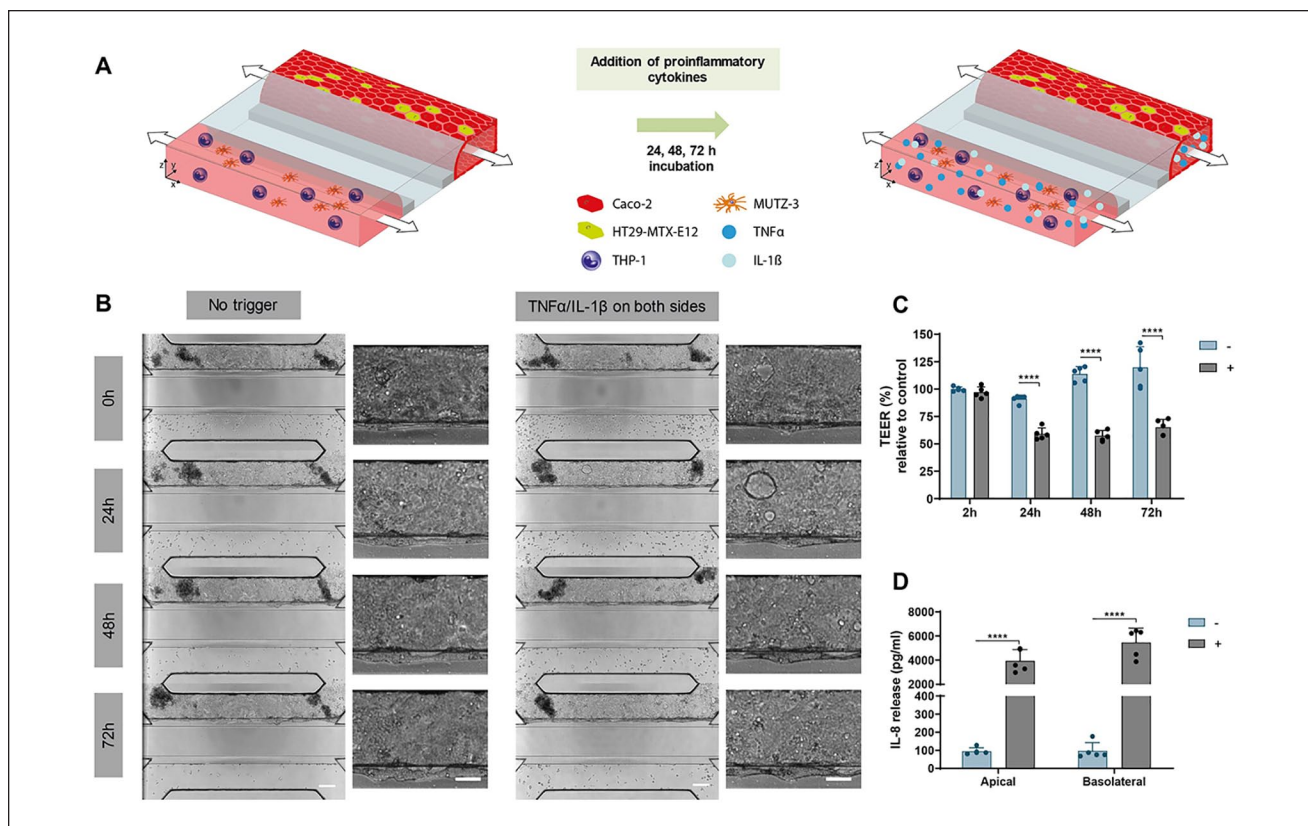
Figure 3. Induction of inflammation in the intestine-on-a-chip model. (**A**) Schematic images showing induction of inflammation in the tetraculture intestinal model in a single chip of the OrganoPlate three-lane upon exposure to TNFα and IL-1β (both at 200 ng/mL) on the apical and basolateral sides. (**B**) Phase-contrast images of the tetraculture model at 4$\times$ or 10$\times$ magnification, showing the effect of TNFα and IL-1β (200 ng/mL, both sides) on the morphology of the cells. (**C**) To determine the effect of the cytokines, TEER of the epithelial barriers was assessed at 2, 24, 48, and 72 h after exposure to the cytokines. Data are represented in percentage and normalized to the 2 h nonexposed condition ($n = 4$). (**D**) Secretion of proinflammatory cytokine IL-8 was assessed in the apical (Caco-2/HT29-MTX) and basolateral (THP-1 and MUTZ-3) compartments in the triggered and nontriggered conditions at 72 h postexposure ($n = 5$). ****$p < 0.0001$. Scale bars in white = 200 or 100 µm for 4$\times$ and 10$\times$ images, respectively.

cells. This effect of TPCA-1 in decreasing IL-8 secretion was observed in both apical and basolateral samples when cultures were exposed to both TNFα and IL-1β. Additionally, another anti-inflammatory compound, budesonide, was tested at different concentrations on the basolateral side of the tetraculture model. The results showed that budesonide had no significant effect on TEER values. However, it caused a decrease in IL-8 secretion in basolateral samples at all concentrations (**Suppl. Fig. S9**). In summary, these results showed that treatment of cultures with the anti-inflammatory compound TPCA-1 can prevent inflammatory status in the cells.

Discussion

In this study, we established a unique intestine-on-a-chip model with biological modularity to study inflammatory processes. By making use of well-established cell lines, we constructed a mucus-producing intestinal tube culture, the complexity of which can be tailored according to the needs of the model. This toolbox allows the development of a complex 3D multicellular model, in which we mimicked intestinal inflammation in the present study, as demonstrated by the loss of barrier function and production of cytokines. Moreover, this simple and reproducible tool kit can be used in its highest (tetraculture) or lowest (coculture) complexity, depending on the research question. This allows robust assays that can serve all preclinical stages in the drug discovery and development process.

The complexity of the model was achieved by creating a tubular structure comprising a coculture of Caco-2 cells and the mucus-producing HT29-MTX-E12 cells against a collagen-I ECM. Additionally, a coculture of the immune-competent THP-1 and MUTZ-3 cells was established by adding the cells to the basal medium compartment. We showed that the Caco-2 and HT29-MTX-E12 coculture formed confluent and polarized tubular structures against the collagen-I ECM in the OrganoPlate, with stable barrier function over
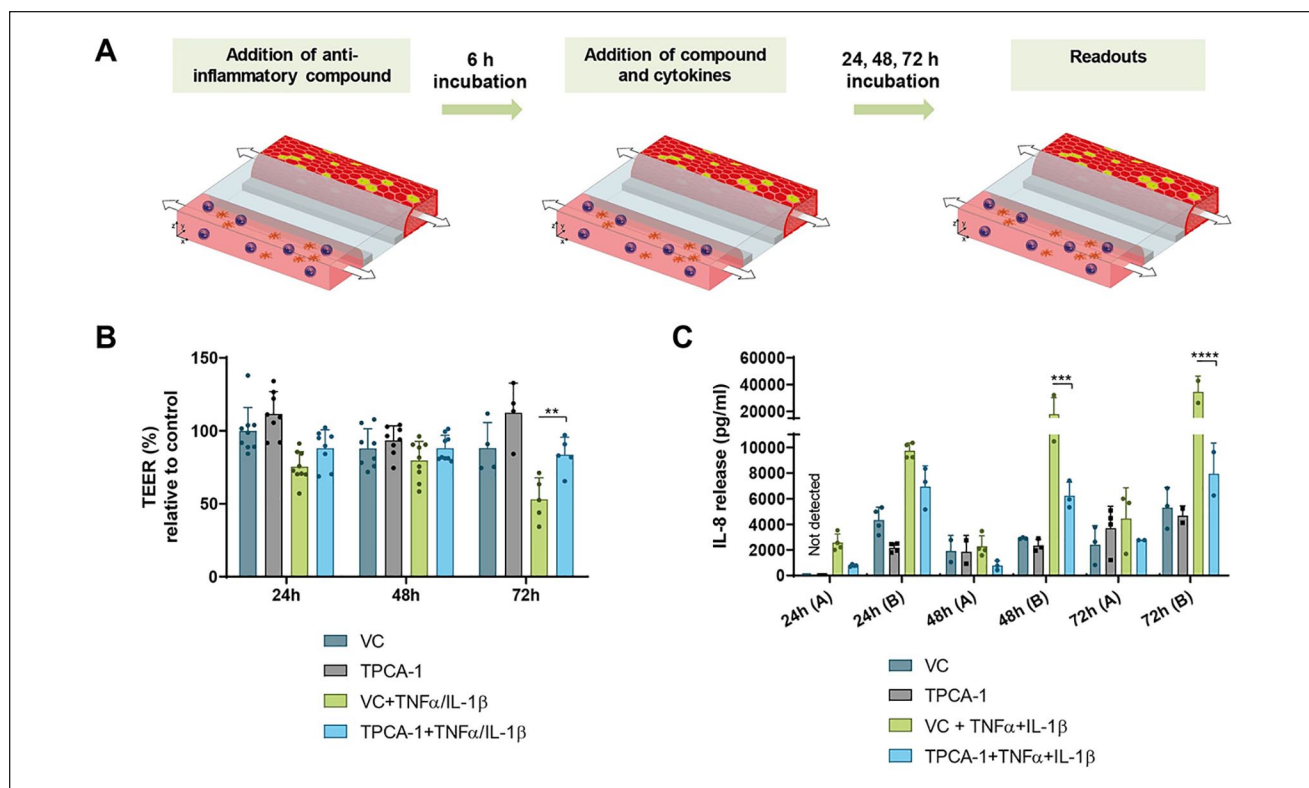
Figure 4. Prevention of the cytokine-induced intestinal inflammation-like phenotype in the intestine-on-a-chip model by addition of the anti-inflammatory compound TPCA-1. (**A**) Schematic overview of the exposure strategy in the tetraculture intestine-on-a-chip model. Cultures were pretreated with 1 μM TPCA-1 and incubated for 6 h under perfusion. Next, the cultures were exposed to TPCA-1 and cytokines (TNFα and/or IL-1β) and incubated on a rocker platform for 24, 48, or 72 h. Finally, the morphology and barrier integrity of the culture as well as cytokine release in the culture were assessed. (**B**) To determine the effect of cytokines and the anti-inflammatory action of TPCA-1 on the culture, TEER of the epithelial barriers was assessed 24, 48, and 72 h after exposure to the cytokines. Data are represented in percentage and normalized to the 24 h nonexposed condition (vehicle control [VC]; n = 4–9 chips). (**C**) Secretion of the proinflammatory cytokine IL-8 was assessed in the (**A**) apical (Caco-2/HT29-MTX) and (**B**) basolateral (THP-1 and MUTZ-3) compartments in the triggered and nontriggered conditions 24, 48, and 72 h after exposure to the cytokines. ***p < 0.001; ****p < 0.0001.

time. We also showed that the model is capable of mucus secretion, as evident from the staining and gene expression analysis results. Mucus is of considerable importance in the gut because it serves as a physical barrier and a way to capture pathogens.[29] Therefore, an in vitro intestinal model containing mucus better reflects the human situation and serves as a better tool for predicting the effect of drugs or pathogens in healthy and disease conditions.

In our system, the cultures are exposed to fluid shear stress through gravity-driven liquid leveling of medium, without the need for pumps or intricate tube systems. Using a defined proinflammatory trigger and immune cells mimicking disease-activated macrophages and dendritic cells, we were able to recapitulate the key characteristics of inflammation in a relevant and reproducible manner. By exposing the cultures to TNFα and/or IL-1β, we were able to induce an inflammatory state, characterized by cytokine release (IL-8) and a decrease in TEER values. As reported

by Singh et al., IBD patients show significantly elevated systemic levels of TNFα and IL-1β relative to healthy subjects,[30] with the former showing average TNFα and IL-1β concentrations of 3000 and 250 pg/mL, respectively. However, it has been shown that systemic concentrations of proinflammatory mediators are much lower than their local tissue levels because of the half-life of cytokines as well as their renal clearance.[31,32] Therefore, systemic cytokine levels cannot serve as representative levels for modeling inflammation in in vitro or in vivo models. Additionally, TNFα and IL-1β proved to be more effective than LPS in activating the epithelium in the present study. The immune cell functionality of the model was determined by exposing monocultures or cocultures of differentiated THP-1 and MUTZ-3 cells to various concentrations of LPS. We observed a concentration- and cell number-dependent increase in IL-8 release by both cells as well as a synergetic effect in the cocultures. This induced inflammatory state of

the cultures in the tetraculture model could be prevented by treatment with the anti-inflammatory compound TPCA-1; this result was evident from the decreased secretion of IL-8 and retention of barrier function in treated cultures at levels similar to those observed in untreated cultures.

Compared with Transwell cultures, other intestine-on-a-chip systems, and animal models, this platform has considerable throughput capacity because of its ability to accommodate 40 independent intestinal cultures in parallel.[16,17] Additionally, the standard 384-well microtiter format of the plate makes it easy to handle, compatible for use within a general cell culture lab, and less consuming in terms of reagents, cells, and time. In addition, organ-on-a-chip systems provide versatile modularity for studying the individual contribution of each factor, thus paving the way toward unraveling the underlying pathophysiology of intestinal inflammation, which is not possible in any animal model. Finally, it is amenable for the pharmaceutical industry to implement microfluidic models in standard drug development processes, as this could lead to an overall reduction of 10%–26% in total costs and save up to 631 million euros for every new drug reaching the market.[33,34] Other microfluidic intestinal models might capture its niche in a certain step of development, but they are lacking intercomparability and overlapping applications. In contrast, the intestine-on-a-chip model in the OrganoPlate supports versatile modularity in capturing intestinal complexity, making it amenable to adoption to all stages of development of novel therapies and preventive agents.

In the present study, TEER measurements provided more sensitive and accurate observations of the changes in barrier integrity of the model than the fluorescent probe (TRITC–dextran) assay. A possible explanation for this is that, while the presence of the mucus layer prevents the fluorescent dye from leaking into the ECM compartment, this is less of a problem for measuring electrical resistance. It has been shown that both pore size and the interaction of the diffusing particle with the mucosal layer determine the permeability of a molecule through the mucus layer.[35,36] Furthermore, TEER measurement demonstrates the ionic conductance of the paracellular and transcellular routes of the epithelium, whereas the flux of a fluorescent dye demonstrates only the paracellular flow of water and the pore size of tight junctions.[37] Finally, for assessing barrier integrity, TEER measurement is preferred over the fluorescent probe assay, because the probe could also interfere with the transport and diffusion of released cytokines and chemokines in the system.[38] TEER measurement is noninvasive and can be applied for monitoring cell growth and differentiation and even the effect of compounds in real time. The nontriggered tetraculture model in the present study showed an increase in TEER over time, indicating improved barrier function. It has been shown that variations in TEER values could arise because of factors such as temperature and cell passage number.[38]

The effect of another anti-inflammatory compound, budesonide, was tested on the tetraculture model. Contrary to the effect of TPCA-1 treatment, budesonide treatment did not prevent an inflammatory state in the culture. Budesonide was added solely on the basolateral side of the culture, whereas TPCA-1 was added on both the apical and basolateral sides. The rationale behind this application was the fact that steroids, such as budesonide, regulate immune response by inducing apoptosis and suppressing proinflammatory cytokines and T-cell proliferation.[39,40] Furthermore, it has been shown that budesonide specifically inhibits the effects of most cytokines produced by macrophages.[41] The direct effect of budesonide on intestinal epithelial cells is not well established but could be of importance in reducing intestinal inflammation.[42] We believe that the current results are interesting for further investigation and, at the same time, demonstrate how such models can be used for assessing anti-inflammatory compounds.

Because the capabilities of the OrganoPlate coculture are vast, the tetraculture biological modular intestinal model presented in this study could be further improved by addition of intestinal microbiota to the lumen of the epithelial tubule, as intestinal microbiota play an important role in maintaining gut homeostasis.[43] Although the use of cell lines allows controlled and reproducible data, it often fails to completely recapitulate in vivo intestinal phenotypes. Alternatively, primary intestinal cells, cells derived from induced pluripotent stem cells (iPSC), and intestinal organoids could serve as sources for increasing the physiological relevance of the model. Ultimately, the organoid or iPSC route can be used to personalize the model for patient stratification and personalized medicine.

In summary, we have developed and characterized a robust, high-throughput, 3D biological modular multicellular perfused intestine-on-a-chip model in which we were able to mimic intestinal inflammation, as demonstrated by the loss of barrier function and production of cytokines. Additionally, this model can be applied for screening anti-inflammatory compounds. Overall, this model allows the versatile modularity of mimicking the key features of intestinal inflammation, which positions it at the forefront of high-throughput screening efforts for supporting drug discovery and providing a platform for personalized medicine.

Acknowledgments

Declaration of Conflicting Interests

ORCID iDs

Diego Marescotti [iD] https://orcid.org/0000-0003-1007-8074

Dorota Kurek [iD] https://orcid.org/0000-0002-7168-8944

References

1. Ng, S. C.; Shi, H. Y.; Hamidi, N.; et al. Worldwide Incidence and Prevalence of Inflammatory Bowel Disease in the 21st Century: A Systematic Review of Population-Based Studies. *Lancet* **2017**, *390*, 2769–2778.
2. Ramos, G. P.; Papadakis, K. A. Mechanisms of Disease: Inflammatory Bowel. *Mayo Clin. Proc.* **2019**, *94*, 155–165.
3. Frank, D. N.; Amand, A. L. S.; Feldman, R. A.; et al. Molecular-Phylogenetic Characterization of Microbial Community Imbalances in Human Inflammatory Bowel Diseases. *Proc. Natl. Acad. Sci. U. S. A.* **2007**, *104*, 13780–13785.
4. Liu, J. Z.; Van Sommeren, S.; Huang, H.; et al. Association Analyses Identify 38 Susceptibility Loci for Inflammatory Bowel Disease and Highlight Shared Genetic Risk across Populations. *Nat. Genet.* **2015**, *47*, 979–986.
5. Ananthakrishnan, A. N. Epidemiology and Risk Factors for IBD. *Nat. Rev. Gastroenterol. Hepatol.* **2015**, *12*, 205–217.
6. Yu, J.; Peng, S.; Luo, D.; et al. In Vitro 3D Human Small Intestinal Villous Model for Drug Permeability Determination. *Biotechnol. Bioengin.* **2012**, *109*, 2173–2178.
7. VanDussen, K. L.; Marinshaw, J. M.; Shaikh, N.; et al. Development of an Enhanced Human Gastrointestinal Epithelial Culture System to Facilitate Patient-Based Assays. *Gut* **2015**, *64*, 911–920.
8. Sinagoga, K. L.; Wells, J. M. Generating Human Intestinal Tissues from Pluripotent Stem Cells to Study Development and Disease. *EMBO J.* **2015**, *34*, 1149–1163.
9. Sato, T.; Clevers, H. Growing Self-Organizing Mini-Guts from a Single Intestinal Stem Cell: Mechanism and Applications. *Science (80-.)* **2013**, *340*, 1190–1194.
10. Schulte, L.; Hohwieler, M.; Müller, M.; et al. Intestinal Organoids as a Novel Complementary Model to Dissect Inflammatory Bowel Disease. *Stem Cells Int.* **2019**, *2019*, 8010645.
11. Kasendra, M.; Tovaglieri, A.; Sontheimer-Phelps, A.; et al. Development of a Primary Human Small Intestine-on-a-Chip Using Biopsy-Derived Organoids. *Sci. Rep.* **2018**, *8*, 1–14.
12. Kim, H. J.; Huh, D.; Hamilton, G.; et al. Human Gut-on-a-Chip Inhabited by Microbial Flora That Experiences Intestinal Peristalsis-Like Motions and Flow. *Lab Chip* **2012**, *12*, 2165–2174.
13. Kim, J. H.; Li, H.; Collins, J. J.; et al. Contributions of Microbiome and Mechanical Deformation to Intestinal Bacterial Overgrowth and Inflammation in a Human Gut-on-a-Chip. *Proc. Natl. Acad. Sci. U. S. A.* **2016**, *13*, E7–E15.
14. Noel, G.; Baetz, N. W.; Staab, J. F.; et al. A Primary Human Macrophage-Enteroid Co-Culture Model to Investigate Mucosal Gut Physiology and Host-Pathogen Interactions. *Sci. Rep.* **2017**, *7*, 1–13.
15. Fois, C. A. M.; Le, T. Y. L.; Schindeler, A.; et al. Models of the Gut for Analyzing the Impact of Food and Drugs. *Adv. Healthc. Mater.* **2019**, *1900968*, 1–23.
16. Trietsch, S. J.; Naumovska, E.; Kurek, D.; et al. Membrane-Free Culture and Real-Time Barrier Integrity Assessment of Perfused Intestinal Epithelium Tubes. *Nat. Commun.* **2017**, *8*, 1–7.
17. Beaurivage, C.; Naumovska, E.; Chang, Y. X.; et al. Development of a Gut-on-a-Chip Model for High Throughput Disease Modeling and Drug Discovery. *Int. J. Mol. Sci.* **2019**, *20*, 5661.
18. Moisan, A.; Michielin, F.; Jacob, W.; et al. Mechanistic Investigations of Diarrhea Toxicity Induced by Anti-HER2/3 Combination Therapy. *Mol. Cancer Ther.* **2018**, *17*, 1464–1474.
19. Vormann, M. K.; Gijzen, L.; Hutter, S.; et al. Nephrotoxicity and Kidney Transport Assessment on 3D Perfused Proximal Tubules. *AAPS J.* **2018**, *20*, 1–11.
20. Ishikawa, T.; Sato, T.; Mohit, G.; et al. Transport Phenomena of Microbial Flora in the Small Intestine with Peristalsis. *J. Theor. Biol.* **2011**, *279*, 63–73.
21. Lentle, R. G.; Janssen, P. W. M. Physical Characteristics of Digesta and Their Influence on Flow and Mixing in the Mammalian Intestine: A Review. *J. Comp. Physiol. B Biochem. Syst. Environ. Physiol.* **2008**, *178*, 673–690.
22. Schindelin, J.; Arganda-Carreras, I.; Frise, E.; et al. Fiji: An Open Source Platform for Biological Image Analysis. *Nat. Methods* **2012**, *9*, 676–682.
23. Hildago, I. J.; Raub, T. J.; Borchardt, R. T. Characterization of the Human Colon Carcinoma Cell Line (Caco-2) as a Model System for Intestinal Epithelial Permeability. *Gastroenterology* **1989**, *96*, 736–749.
24. Lesuffleur, T.; Porchet, N.; Aubert, J.; et al. Differential Expression of the Human Mucin Genes MUC1 to MUC5 in Relation to Growth and Differentiation of Different Mucus-Secreting HT-29 Cell Subpopulations. *J. Cell Sci.* **1993**, *106*, 771–783.
25. Steinbach, E. C.; Plevy, S. E. The Role of Macrophages and Dendritic Cells in the Initiation of Inflammation in IBD. *Inflamm. Bowel Dis.* **2014**, *20*, 166–175.
26. Masterson, A. J.; Sombroek, C. C.; De Gruijl, T. D.; et al. MUTZ-3, a Human Cell Line Model for the Cytokine-Induced Differentiation of Dendritic Cells from CD34+ Precursors. *Blood* **2002**, *100*, 701–703.
27. Műzes, G.; Molnár, B.; Tulassay, Z.; et al. Changes of the Cytokine Profile in Inflammatory Bowel Diseases. *World J. Gastroenterol.* **2012**, *18*, 5848–5861.
28. Murch, S. H.; Braegger, C. P.; Walker-Smith, J. A.; et al. Location of Tumour Necrosis Factor α by Immunohistochemistry in Chronic Inflammatory Bowel Disease. *Gut* **1993**, *34*, 1705–1709.

29. Navabi, N.; McGuckin, M. A.; Lindén, S. K. Gastrointestinal Cell Lines Form Polarized Epithelia with an Adherent Mucus Layer When Cultured in Semi-Wet Interfaces with Mechanical Stimulation. *PLoS One* **2013**, *8*.

30. Singh, U. P.; Singh, N. P.; Murphy, E. A.; et al. Chemokine and Cytokine Levels in Inflammatory Bowel Disease Patients. *Cytokine* **2016**, *77*, 44–49.

31. Goris, R. J. A. Local versus Systemic Inflammatory Responses in Shock, Trauma and Sepsis. *Int. J. Intensive Care* **1999**, *6*, 81–90.

32. Holzheimer, R.; Steinmetz, W. Local and Systemic Concentrations of Pro- and Anti-Inflammatory Cytokines in Human Wounds. *Eur. J. Med. Res*. **2000**, *5*, 347–355.

33. DiMasi, J. A.; Grabowski, H. G.; Hansen, R. W. Innovation in the Pharmaceutical Industry: New Estimates of R&D Costs. *J. Health Econ*. **2016**, *47*, 20–33.

34. Adams, C. P.; Brantner, V. V. Spending on New Drug Development. *Health Econ*. **2010**, *19*, 130–141.

35. Macierzanka, A.; Böttger, F.; Rigby, N. M.; et al. Enzymatically Structured Emulsions in Simulated Gastrointestinal Environment: Impact on Interfacial Proteolysis and Diffusion in Intestinal Mucus. *Langmuir* **2012**, *28*, 17349–17362.

36. Macierzanka, A.; Rigby, N. M.; Corfield, A. P.; et al. Adsorption of Bile Salts to Particles Allows Penetration of Intestinal Mucus. *Soft Matter* **2011**, *7*, 8077–8084.

37. Zucco, F.; Batto, A. F.; Bises, G.; et al. An Inter-Laboratory Study to Evaluate the Effects of Medium Composition on the Differentiation and Barrier Function of Caco-2 Cell Lines. *Altern. Lab. Anim*. **2005**, *33*, 603–618.

38. Srinivasan, B.; Kolli, A. R.; Esch, M. B.; et al. TEER Measurement Techniques for In Vitro Barrier Model Systems. *J. Lab. Autom*. **2015**, *20*, 107–126.

39. Oddera, S.; Silvestri, M.; Sacco, O.; et al. Evaluation of the Inhibitory Effects of Budesonide on the Mitogen-Induced or the Allergen-Induced Activation of Blood Mononuclear Cells Isolated from Asthmatic Patients. *Ann. Allergy. Asthma Immunol*. **1995**, *75*, 33–40.

40. Waage, A.; Bakke, O. Glucocorticoids Suppress the Production of Tumour Necrosis Factor by Lipopolysaccharide-Stimulated Human Monocytes. *Immunology* **1988**, *63*, 299–302.

41. Schmidt, M.; Pauels, H. G.; Lügering, N.; et al. Glucocorticoids Induce Apoptosis in Human Monocytes: Potential Role of IL-1 Beta. *J. Immunol*. **1999**, *163*, 3484–3490.

42. Fredin, M. F.; Ulfhammer, E.; Rhedin, M.; et al. Anti-Inflammatory Effects of Budesonide in Intestinal Epithelial Cells. *Pharmacol. Res*. **2005**, *52*, 422–428.

43. Round, J. L.; Mazmanian, S. K. The Gut Microbiota Shapes Intestinal Immune Responses during Health and Disease. *Nat. Rev. Immunol*. **2009**, *9*, 313–323.